

Letters

Surface property study of additively manufactured Inconel 625 at room temperature and 510 °C

Manisha Tripathy ^{a,1}, Michael Munther ^{b,1}, Keivan Davami ^{b,*}, Ali Beheshti ^{a,*}^a Department of Mechanical Engineering, George Mason University, Fairfax, VA, USA^b Department of Mechanical Engineering, University of Alabama, Tuscaloosa, AL, USA

ARTICLE INFO

Article history:

Received 15 June 2020

Received in revised form 19 September

2020

Accepted 16 October 2020

Available online 3 November 2020

Keywords:

Inconel 625

Additive manufacturing

High temperature

Nanoindentation

Friction and wear

ABSTRACT

Various mechanical systems are subjected to inherent oscillatory motions often paired with extreme, high-temperature environments resulting in fretting wear. In this work, the fretting wear resistance of additively manufactured Inconel 625 was studied at room and elevated temperatures. In-situ temperature-controlled nanoindentation was employed to further elucidate mechanical property evolution as a function of temperature. The results showed a 30% decrease in near-surface mean hardness at 510 °C compared to room temperature. However, the material exhibited significantly lower wear and coefficient of friction values at high temperatures, attributed to the formation of a compacted, intermediate oxide layer preventing excessive friction and wear.

© 2020 Society of Manufacturing Engineers (SME). Published by Elsevier Ltd. All rights reserved.

1. Introduction

Nickel-based superalloys with superior thermochemical, mechanical, and tribological properties are of high importance for critical components in several applications such as gas turbine engines, propulsion shafts, welding products, and heat exchangers [1–4]. Such components are usually under inherent vibration leading to small amplitude displacements under normal pressure at interfaces which leads to a phenomenon called fretting wear [5]. Fretting wear is defined as wear arising due to the linear oscillating motion of relatively small amplitudes [6–8]. While wear and corrosion have been studied extensively for Inconel 625 coatings [9–13], there is a scarcity of available studies in the area of fretting/sliding wear of traditionally manufactured Inconel 625 components [14,15]. With additive manufacturing gaining traction in the modern manufacturing sector on a daily basis, interest has peaked among researchers to replace the conventional manufacturing process with additively-manufactured (AM) materials. There has been an extensive number of studies on discrete aspects of the AM Inconel 625 such as surface morphology [16–18], mechanical behavior [19–21], and microstructural evolution [22–24]. However,

limited investigations are available in tribological aspects [25,26] with no available study on contact behavior and fretting wear of AM Inconel 625 at high temperatures. Industrial applications of grade 1 Inconel 625 [27] such as in feedstock stock superheaters [28], flexible couplings in automotive exhaust systems [2], and many more applications generally operating between 400 °C and 650 °C are potential applications for future AM Inconel 625 adoption. This report attempts to achieve this goal by performing fretting wear tests at room temperature and 510 °C using a silicon nitride ball (as counterpart) on AM Inconel 625 paired with in-situ temperature-controlled indentation to study the evolution of surface mechanical properties correlating with temperature rise.

2. Experimental setup

The fretting tests were conducted using Bruker UMT-TriboLab consisted of an upper assembly with a carriage and pin holder and a lower assembly comprising of a drive and sample holder along with a temperature chamber as shown in Fig. 1(a). The carriage is mounted with a force sensor that can measure normal and lateral forces up to 200 N (Fig. 1(b)). The reciprocating drive was used to simulate a linear oscillatory motion capable of a stroke length of 0.1–25 mm with a frequency of up to 60 Hz. (details in supplementary information (SI) section S1).

^{*} Corresponding authors.E-mail addresses: kdavami@eng.ua.edu (K. Davami), abehesh@gmu.edu (A. Beheshti).¹ These authors contributed equally.

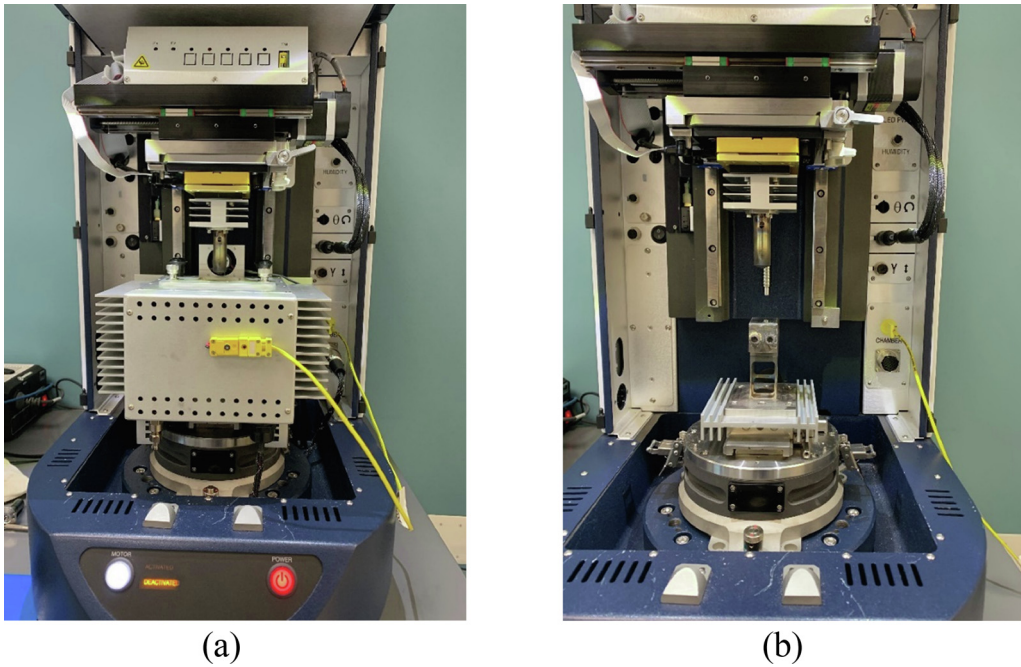


Fig. 1. Bruker UMT-TriboLab (a) with the temperature chamber, (b) without the temperature chamber.

3. Results and discussion

3.1. Fretting wear

Fig. 2(a) shows the representative in-situ coefficient of friction (CoF) with respect to time at room and 510 °C temperatures. The friction at room temperature begins at approximately 0.4 and fluctuates before it achieves steady-state at a value of 0.49. The fluctuations can be attributed to the initial running-in process with thin oxide layer removal as well as generation and accumulation of a high amount of debris in the contact area while surface asperities become truncated. This results in an increase in the contact area, leading to a relatively stable CoF. At an elevated temperature of 510 °C, fairly moderate fluctuations are observed, wherein the CoF begins at 0.35 and eventually reaches a steady-state value of 0.26. High consistency was observed between two test trials wherein an averaged steady-state CoF is found to be 0.48 at room temperature and 0.26 at 510 °C (**Fig. 2(b)**). At high temperature, CoF stabilizes in a shorter time (~500 s) as compared to the room temperature experiment (~1400 s). These COF values were compared and found to be in line with the behavior of the wrought Inconel 625 investigated by Iwabuchi [14]. The low fluctuations, rapid stabilization, as well as lower CoF at elevated temperatures, can be mainly attributed to the formation of a glazed compacted oxide layer on the surface. The compacted oxide layer starts to form as the experiment begins where it becomes more uniform over time leading to a stable CoF. This stable, glazed layer acts as a lubricating protective intermediate layer separating direct contact ball-on-substrate thus reducing the friction between the contacting surfaces. The formation of this glazed layer has been observed for several nickel-based alloys including previous studies of the authors [14,29–35]. The SEM images (see **Fig. S2** of SI) show the relatively uniform layer formed by the compaction of the wear debris trapped in the contact for the 510 °C track in contrast to distinct ploughing lines seen in the room temperature track. In addition, and to a lesser extent, stable and low CoF observation can be attributed to the increase in bulk material compliance at high temperatures (see Section 3.2) making the contact more conformal,

reducing local pressure, and thus decreasing resistant to the motion, and subsequently lowering deformation (ploughing) component of CoF that results in an overall smaller CoF.

Fig. 3(a) and (b) display representative wear scars for tests at room temperature and 510 °C, respectively. **Fig. 2(c)** and (d) show the maximum wear depth as well as wear volume for all the tests as well as the mean values. At room temperature, the maximum wear depth is higher than that of 510 °C. Similarly, the calculated wear volume at room temperature is about $14,970 \mu\text{m}^3$ where at 510 °C, it reduces to $6420 \mu\text{m}^3$. The observation of lower wear at elevated temperatures is similar to the trend found for CoF. This tribological behavior was also observed by Iwabuchi [14] for wrought Inconel 625 and also in other nickel-based alloys [29–32,36–38] including studies by the authors (Inconel 617 [34] and Incoloy 800H [35]). At 510 °C, the oxidation rate becomes considerable compared to room temperature due to the presence of sufficient air and an oxide layer forms on nickel-based alloys. This top layer mainly consists of nickel oxide and chromium oxide [33–35]. At high temperatures with sufficient contact pressure, oxide particles form a stable 'compacted glazed oxide' layer with good adhesion to the substrate which decreases the wear volume on the track [39] and acts as an intermediate protective layer between the silicon nitride ball and the substrate. This reduces direct contact with the substrate and mitigates the excessive amount of wear.

3.2. Nanoindentation

Fig. 4 displays both hardness and Young's Modulus of the material at room temperature and 510 °C. Seven individual trials were conducted for each temperature regime wherein curve-fitting of the force–displacement curves was performed using the Oliver-Pharr method to extract relevant hardness and modulus information [40]. It can be seen that mean surface hardness and modulus decrease from 4.85 GPa to 3.49 GPa, and 203.50 GPa to 138.59 GPa as temperature increases from room temperature to 510 °C, which is in agreement with other reports elucidating the high-temperature deformation of Ni-based superalloys [41,42]. This

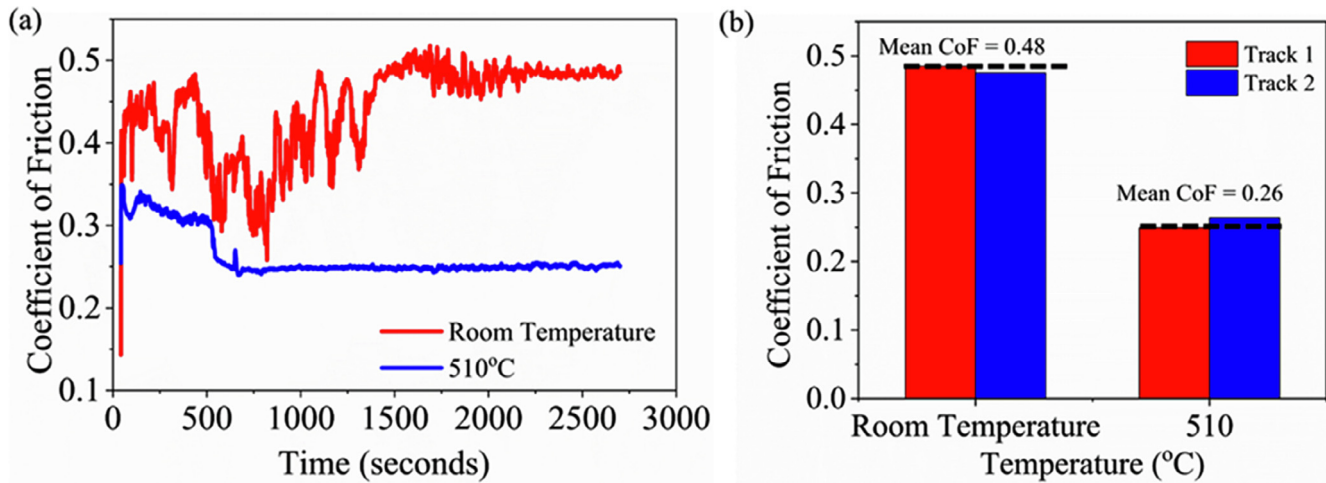


Fig. 2. (a) In-situ CoF and (b) average CoF for room and high-temperature conditions.

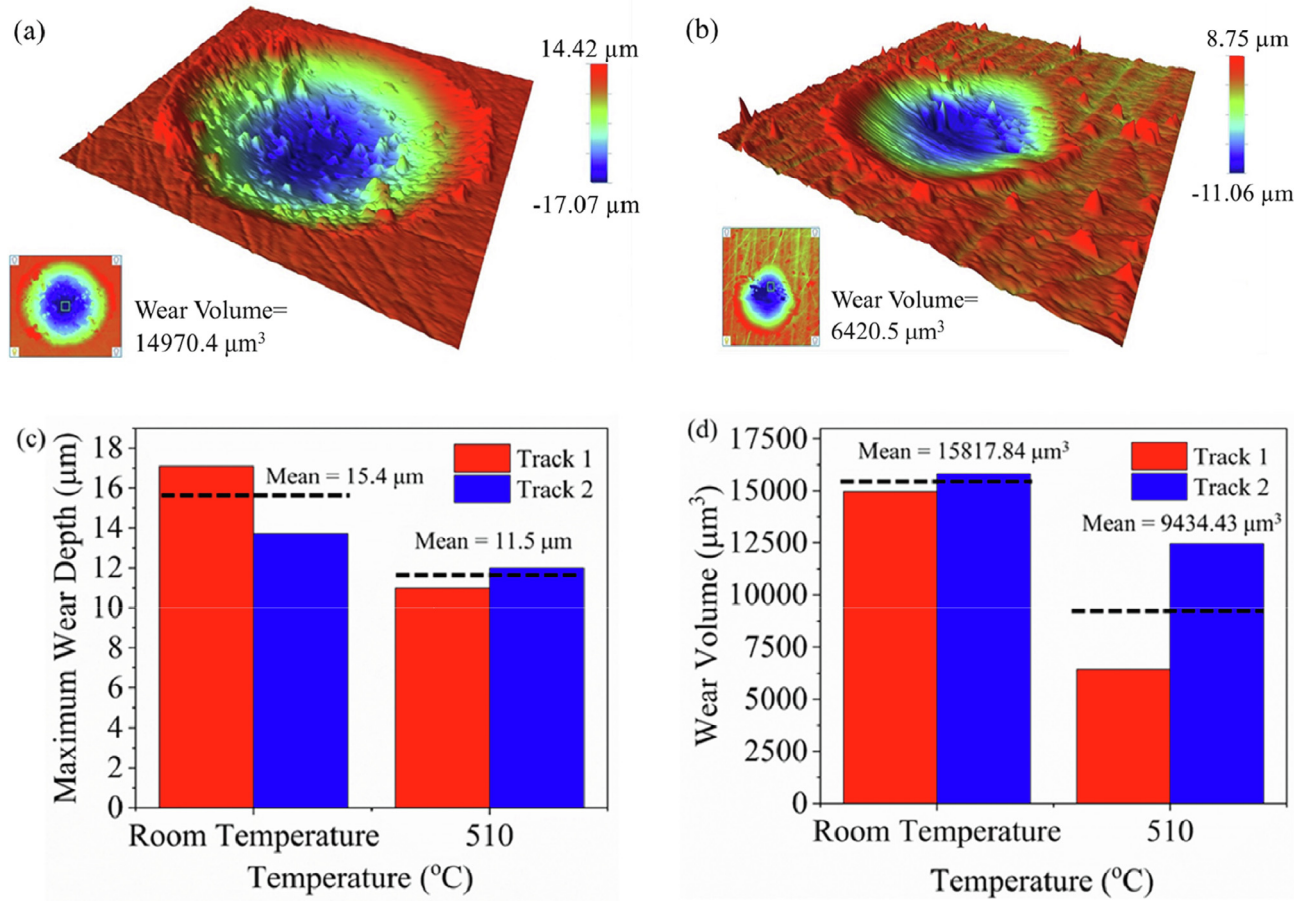


Fig. 3. Wear scars at (a) room temperature and (b) 510 °C; (c) maximum wear depth and (d) wear volume versus temperature.

observed reduction in both surface hardness and modulus is mainly attributed to the softening effect as a result of heat input. Specifically, in several variants of Inconel, it has been observed that moderate heat input in a short duration of time significantly overshadows the effect the strengthening phases, which ultimately increases ductility, making the material more susceptible to deformation [43]. It should be also added that 510 °C, is a low temperature for precipitation hardening to occur in Inconel 625 [44]. It

should be noted that this does not necessarily mean higher wear volume at elevated temperatures, as the oxide formulation is the most important factor to influence a tribo-pair behavior. Due to the formation of the compacted oxide layer, the increase in ductility does not influence the high-temperature wear behavior of AM Inconel 625 as characterized by the results presented in Figs. 2 and 3. Additional indentation results are illustrated in the Supplementary Information section S2.

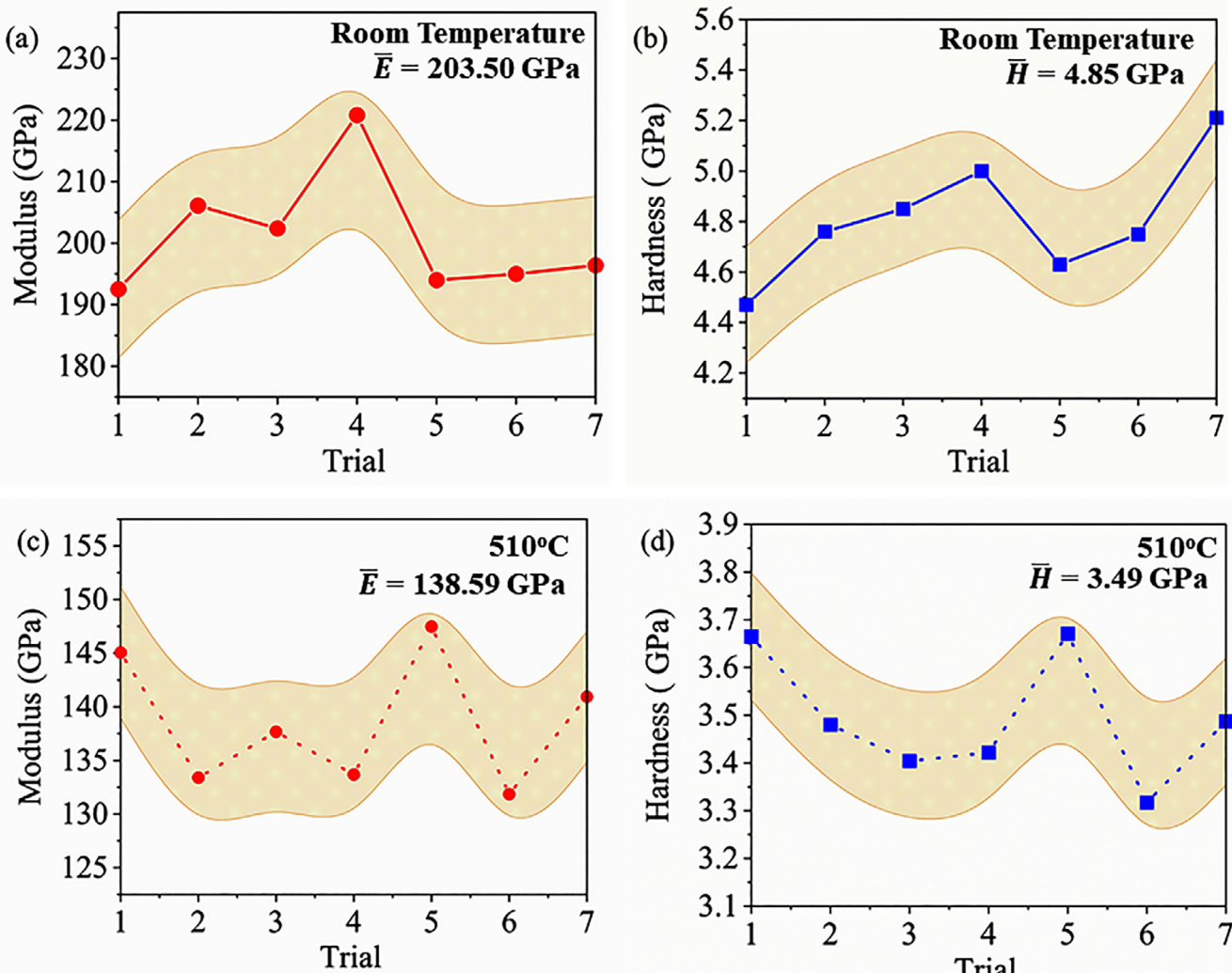


Fig. 4. Nanomechanical characterization of Inconel 625: (a) Young's Modulus and (b) hardness at room temperature, (c) Young's Modulus and (d) hardness at 510 °C. Error curves represent the standard deviation from each respective measurement.

4. Conclusion

Fretting wear tests coupled with in-situ temperature-controlled indentation were conducted on AM Inconel 625 at room temperature and 510 °C to establish its tribological and mechanical behaviors at elevated temperatures. While hardness and elastic modulus reduced significantly at 510 °C, the coefficient of friction and wear were found to be lower at 510 °C compared to room temperature tests. This is due to the formation of a compacted oxide layer acting as a lubricating stopgap layer minimizing direct contact between the ball and the substrate, reducing wear at elevated temperature. This report presents the first elevated temperature study on AM Inconel 625 and is a path forward to its effective incorporation in novel designs and complex components in many applications.

Declaration of Competing Interest

The authors declare that they have no known competing financial interests or personal relationships that could have appeared to influence the work reported in this paper.

Acknowledgments

The authors would like to thank Dr. Marzyeh Moradi (KLA) for her work in conducting the nanoindentation measurements pre-

sented. The support of KLA and ICMAS Inc. is acknowledged. The authors would like also to thank John Laureto and Keith Brady from Renishaw for providing the AM samples. Authors, M.M. and K.D. extend gratitude to the Alabama Transportation Institute (ATI) for their support of the graduate student involved in this work, as well as the Advanced Manufacturing program of National Science Foundation (NSF) with award number CMMI-AM #2029059.

Appendix A. Supplementary data

Supplementary data to this article can be found online at <https://doi.org/10.1016/j.mfglet.2020.10.001>.

References

- [1] Shoemaker LE. Alloys 625 and 725: trends in properties and applications. In: Proc. Int. Symp. Superalloys Var. Deriv.. p. 409–18.
- [2] Smith GD, Tillack DJ, Patel SJ. Alloy 625 – Impressive Past/Significant Presence/Awesome Future.
- [3] Ganeshan P, Renteria CM, Crum JR. Versatile corrosion resistance of INCONEL alloy 625 in various aqueous and chemical processing environments.
- [4] Cuevas-Arteaga C, Verhelst D, Alfantazi A. Performance of alloy 625 under combustion gas environments-A review.
- [5] Madge JJ, Leen SB, Shipway PH. The critical role of fretting wear in the analysis of fretting fatigue. Wear, 263(1–6 Spec. Iss.), (2007) 542–551.
- [6] Hoepner D, Chandrasekaran V. Frett Fatigue Curr Technol Pract 2000.

[7] Berthier Y, Vincent L, Godet M. Fretting fatigue and fretting wear. *Tribol Int* 1989;22(4):235–42.

[8] Waterhouse RB. Fretting wear. *Wear* 1984;100(1–3):107–18.

[9] Zhang D, Harris SJ, McCartney DG. Microstructure formation and corrosion behaviour in HVOF-sprayed Inconel 625 coatings. *Mater Sci Eng, A* 2003;344(1–2):45–56.

[10] Tuominen J, Vuoristo P, Mäntylä T, Latokartano J, Vihtinen J, Andersson PH. Microstructure and corrosion behavior of high power diode laser deposited Inconel 625 coatings. *J Laser Appl* 2003;15(1):55–61.

[11] Al-Fadhl HY, Stokes J, Hashmi MSJ, Yilbas BS. HVOF coating of welded surfaces: Fatigue and corrosion behaviour of stainless steel coated with Inconel-625 alloy. *Surf Coat Technol* 2006;200(16–17):4904–8.

[12] Chaudhuri A, Raghupathy Y, Srinivasan D, Suwas S, Srivastava C. Microstructural evolution of cold-sprayed Inconel 625 superalloy coatings on low alloy steel substrate. *Acta Mater* 2017;129:11–25.

[13] Chen TC, Chou CC, Yung TY, Tsai KC, Huang JY. Wear behavior of thermally sprayed Zn/15Al, Al and Inconel 625 coatings on carbon steel. *Surf Coat Technol* 2016;303:78–85.

[14] Iwabuchi A. Fretting wear of Inconel 625 at high temperature and in high vacuum. *Wear* 1985;106(1–3):163–75.

[15] Vermeulen M. Wear research on large-scale test specimen. *Wear* 1989;132(2):287–302.

[16] Mumtaz K, Hopkinson N. Selective laser melting of Inconel 625 using pulse shaping.

[17] Mumtaz K, Hopkinson N. Top surface and side roughness of Inconel 625 parts processed using selective laser melting. *Rapid Prototyp J* 2009;15(2):96–103.

[18] Gan Z, Lian Y, Lin SE, Jones KK, Liu WK, Wagner GJ. Benchmark study of thermal behavior, surface topography, and dendritic microstructure in selective laser melting of Inconel 625. *Integr Mater Manuf Innov* 2019;8(2):178–93.

[19] Hack H, Link R, Knudsen E, Baker B, Olig S. Mechanical properties of additive manufactured nickel alloy 625. *Addit Manuf* 2017;14:105–15.

[20] Kreitberg A, Brailovsky V, Turenne S. Elevated temperature mechanical behavior of IN625 alloy processed by laser powder-bed fusion. *Mater Sci Eng, A* 2017;700:540–53.

[21] ASTM, ASTM G204: Standard Test Method for Damage to Contacting Solid Surfaces under Fretting Conditions, ASTM Stand, vol. i, pp. 1–5, 2010.

[22] Amato K. Comparison of microstructures and properties for a Ni-base superalloy (alloy 625) fabricated by electron beam melting. *J Mater Sci Res* 2012;1(2):3.

[23] Li C, Guo YB, Zhao JB. Interfacial phenomena and characteristics between the deposited material and substrate in selective laser melting Inconel 625. *J Mater Process Technol* 2017;243:269–81.

[24] Li S, Wei Q, Shi Y, Chua CK, Zhu Z, Zhang D. Microstructure characteristics of Inconel 625 superalloy manufactured by selective laser melting. *J Mater Sci Technol* 2015;31(9):946–52.

[25] Anil PM, Naiju CD. Sliding wear reliability studies of Inconel 625 components manufactured by direct metal deposition (DMD). *Procedia Manuf* 2019;30:581–7.

[26] Gao Y, Zhou M. Superior mechanical behavior and fretting wear resistance of 3D-printed Inconel 625 superalloy. *Appl Sci* 2018;8(12):2439.

[27] N. Alloys, C. Alloys, H. Alloys, Standard specification for nickel-chromium-molybdenum-columbium alloy and nickel-chromium-molybdenum-silicon alloy plate, sheet, and, pp. 1–8, 2019.

[28] Thomas C, Tait P. The performance of Alloy 625 in long-term intermediate temperature applications. *Int J Press Vessel Pip* 1994;59(1–3):41–9.

[29] Birol Y. High temperature sliding wear behaviour of Inconel 617 and Stellite 6 alloys. *Wear* 2010;269(9–10):664–71.

[30] Radu I, Li DY. Investigation of the role of oxide scale on Stellite 21 modified with yttrium in resisting wear at elevated temperatures. *Wear* 2005;259(1–6):453–8.

[31] Stott FH. High-temperature sliding wear of metals. *Tribol Int* 2002;35(8):489–95.

[32] Stott FH, Lin DS, Wood GC. The structure and mechanism of formation of the 'glaze' oxide layers produced on nickel-based alloys during wear at high temperatures. *Corros Sci* 1973;13(6):449–69.

[33] Rahman MS, Ding J, Beheshti A, Zhang X, Polycarpou AA. Elevated temperature tribology of Ni alloys under helium environment for nuclear reactor applications. *Tribol Int* 2018;123:372–84.

[34] Rahman MS, Ding J, Beheshti A, Zhang X, Polycarpou AA. Helium tribology of Inconel 617 at elevated temperatures up to 950°C: parametric study. *Nucl Sci Eng* 2019;193(9):998–1012.

[35] Rahman MS, Ding J, Beheshti A, Zhang X, Polycarpou AA. Tribology of incoloy 800HT for nuclear reactors under helium environment at elevated temperatures. *Wear* 2019;436:436–437.

[36] Blau PJ. Elevated-temperature tribology of metallic materials. *Tribol Int* 2010;43(7):1203–8.

[37] Stott FH. The role of oxidation in the wear of alloys. *Tribol Int* 1998;31(1–3):61–71.

[38] Chen TC, Chou CC, Yung TY, Cai RF, Huang JY, Yang YC. A comparative study on the tribological behavior of various thermally sprayed Inconel 625 coatings in a saline solution and deionized water. *Surf Coat Technol* 2020;385:125442.

[39] Waterhouse RB, Iwabuchi A. High temperature fretting wear of four titanium alloys. *Wear* 1985;106(1–3):303–13.

[40] Oliver WC, Pharr GM. An improved technique for determining hardness and elastic modulus using load and displacement sensing indentation experiments. *J Mater Res* 1992;7(06):1564–83.

[41] Zhang Y, Mohanty DP, Seiler P, Siegmund T, Kružic JJ, Tomar V. High temperature indentation based property measurements of IN-617. *Int J Plast* 2017;96:264–81.

[42] Salari S, Rahman MS, Polycarpou AA, Beheshti A. Elevated temperature mechanical properties of Inconel 617 surface oxide using nanoindentation. *Mater Sci Eng, A* 2020;788:139539.

[43] Xue H, Lijun W, Hui X, Runguang L, Shaogang W, Zhonglin C. Superplastic properties of Inconel 718, *J Mater Process Technol*, 137(1–3) SPEC, 2003, 17–20.

[44] Shaikh MA, Ahmad M, Shoaib KA, Akhter JI, Iqbal M. Precipitation hardening in Inconel 625. *Mater Sci Technol* 2000;16(2):129–32.